


Ferromagnetism and its stability from the one-magnon spectrum in twisted bilayer graphene

Yahya Alavirad and Jay Sau

Department of Physics, Condensed Matter Theory Center and the Joint Quantum Institute, University of Maryland, College Park, Maryland 20742, USA (Received 27 September 2019; revised 2 September 2020; accepted 12 October 2020; published 11 December 2020)

We study ferromagnetism and its stability in twisted bilayer graphene. We work with a Hubbard-like interaction that corresponds to the screened Coulomb interaction in a well-defined limit where the Thomas-Fermi screening length l_{TF} is much larger than monolayer graphene's lattice spacing $l_g \ll l_{\text{TF}}$ and much smaller than the moiré superlattice's spacing $l_{\text{TF}} \ll l_{\text{moiré}}$. We show that in the perfectly flat band “chiral” limit and at filling fractions $\pm 3/4$, the saturated ferromagnetic (spin- and valley-polarized) states are ideal ground-state candidates in the large band-gap limit. By assuming a large enough substrate (hBN) induced sublattice potential, the same argument can be applied to filling fractions $\pm 1/4$. We estimate the regime of stability of the ferromagnetic phase around the chiral limit by studying the exactly calculated spectrum of one-magnon excitations. The instability of the ferromagnetic state is signaled by a negative magnon excitation energy. This approach allows us to deform the results of the idealized chiral model (by increasing the bandwidth and/or modified interactions) toward more realistic systems. Furthermore, we use the low-energy part of the exact one-magnon spectrum to calculate the spin-stiffness of the Goldstone modes throughout the ferromagnetic phase. The calculated value of spin-stiffness can determine the excitation energy of charged skyrmions.

DOI: [10.1103/PhysRevB.102.235123](https://doi.org/10.1103/PhysRevB.102.235123)**I. INTRODUCTION**

Ferromagnetism is the most familiar form of magnetic order. Despite the long history of ferromagnetism, most of our current understanding is based on simple Hartree-Fock (mean-field) calculations [1]. These calculations are known to greatly overestimate the ferromagnetic tendency of electronic systems. Several improvements over the Hartree-Fock method have been proposed [2,3]. Yet, the overall progress in this direction has not led to a theory that provides reliable diagnostics for which systems would be ferromagnetic.

A useful practical guide is provided by the Hund's rule, which predicts ferromagnetic spin polarization in partially filled degenerate sets of energy states (orbitals). Specifically, the exchange term in the Coulomb interaction reduces the Coulomb repulsion between electrons of similar spin-favoring spins to align with each other. Interestingly, the same general principle appears to apply to quantum Hall ferromagnetism. In both of these cases, the degeneracy of the noninteracting energy eigenstates seems essential to enhance the effect of the ferromagnetic exchange [4].

While a faithful treatment of magnetism in electronic systems is complicated, the limit of strong on-site Coulomb interaction U , the so-called Hubbard interaction [5], has been demonstrated to lead to antiferromagnetic Néel order on an energy-scale proportional to Heisenberg superexchange [1]. The magnetic order has been shown to flip to ferromagnetism in the limit of exactly one-hole and infinite on-site repulsion U [6–8]. These results were extended by Lieb to the half-filled Hubbard model with an imbalance in the number of sublattices [9], establishing the possibility of itinerant

ferrimagnetism. These ideas of enhancement of magnetism by local interaction and of ferromagnetism by degeneracy of noninteracting states were later shown to reinforce each other through the demonstration of ferromagnetism in half-filled lattice models with Hubbard interactions that have a degenerate manifold of states in the form of a flatband [4,10–21]. The latter class of results constitute what is usually called “flatband ferromagnetism.”

Despite the large variety of theoretical models demonstrating spontaneous ferromagnetism as well as competing magnetic and itinerant phases, solid-state realizations of such models are not commonplace. Recent experimental breakthroughs in the area of multilayer graphene both in the quantum Hall regime and without magnetic fields provide hope for the realization of such systems. In the quantum Hall regime, graphene provides the opportunity to break the flatness of a Landau level by introducing a lattice potential on the scale of a magnetic length that has been shown to create a Hofstadter spectrum [22]. Based on arguments in the previous paragraphs, one expects such a broadening of the Landau levels to compete with quantum Hall ferromagnetism in an interesting way. The latter case of multilayer graphene without a magnetic field is a more unexpected direction and appears to have evidence for ferromagnetism. More specifically, large peaks in the density of states associated with nearly flatbands and the concomitant appearance of correlated phenomena have recently been observed in twisted bilayer, twisted double-bilayer, and ABC trilayer graphene [23–35]. Some of these systems have also shown evidence for ferromagnetism [28,30–33,35] near the “flatband” limit.

Additionally, the possibility of tuning these systems out of the “flatband” regime suggests the fascinating possibility of studying multiple phases and transitions between them of insulating and itinerant magnetic systems.

In this work, we consider the particular example of twisted-bilayer graphene (TBLG). We start by focusing on the so-called “chiral” limit of the realistic models for TBLG, where the spectrum supports a band that is exactly flat [36–38]. We work with a particular form of Hubbard interaction that we argue can emerge from Thomas-Fermi screening of the Coulomb interaction. We then show that in this limit and at filling fractions $\pm 3/4$, the saturated spin- and valley-polarized states are ideal ground-state candidates of the system. By assuming a large enough substrate (hBN) induced sublattice potential, the same argument can be shown to hold for filling fractions $\pm 1/4$. The topology of the TBLG band structure guarantees that all the ferromagnetic states discussed above are also associated with a quantized anomalous Hall response [39,40]. We study the local stability of the ferromagnetic phase around the chiral limit by studying the *exactly* calculated spectrum of one-magnon excitations. The instability of the ferromagnetic state is signaled by a negative magnon excitation energy. This approach allows us to deform the results from the idealized chiral model (by increasing the bandwidth and/or modified interactions) toward results for more realistic systems. We use the low-energy part of the exact one-magnon spectrum to predict the spin stiffness of the Goldstone modes in the ferromagnetic phase as the realistic system is approached. The effect of spin stiffness can be potentially determined from skyrmion-induced transport phenomena.

II. BAND STRUCTURE OF TBLG

TBLG corresponds to two layers of graphene stacked on top of each other with a relative twist angle θ . For small twist angles θ , and within the leading harmonic approximation, this system forms a periodic pattern called a moiré pattern. In this limit, the noninteracting physics can be well approximated by the Bistritzer and Macdonald continuum model [41,42]. Following the notation of Ref. [43], the dimensionless single valley ($\zeta = \pm 1$ is the valley index) Bistritzer and Macdonald Hamiltonian can be written in the layer (1,2) and sublattice (A, B) basis (A_1, B_1, A_2, B_2) as

$$H_{\text{BM}}^{\zeta} = \begin{pmatrix} H_1 & U^{\dagger}(\mathbf{r}) \\ U(\mathbf{r}) & H_2 \end{pmatrix}, \quad (1)$$

where

$$H_l = -R(\pm\theta/2)(k - K_{\zeta}^l)(\zeta\sigma_x, \sigma_y) + \Delta_l\sigma_z \quad (2)$$

and

$$U(\mathbf{r}) = \begin{pmatrix} \alpha_0 & \alpha_1 \\ \alpha_1 & \alpha_0 \end{pmatrix} + \begin{pmatrix} \alpha_0 & \alpha_1 e^{-2\pi i\zeta/3} \\ \alpha_1 e^{2\pi i\zeta/3} & \alpha_0 \end{pmatrix} e^{i\zeta G_1 r} \\ + \begin{pmatrix} \alpha_0 & \alpha_1 e^{2\pi i\zeta/3} \\ \alpha_1 e^{-2\pi i\zeta/3} & \alpha_0 \end{pmatrix} e^{i\zeta(G_1+G_2)r}. \quad (3)$$

Here, G 's are the reciprocal-lattice vectors of the moiré lattice, and K_{ζ}^l 's are the location of monolayer Dirac points in the Brillouin zone. Δ_l 's are the (hBN) induced sublattice poten-

tials. In monolayer graphene, Δ is known to be able to reach around $\Delta \approx 0.1\text{--}0.15$ (in dimensionless units used here or equivalently 15–30 meV) [44–46].

The dimensionless parameters α_0, α_1 are given by

$$\alpha_0 = \frac{3w_{AB}a_0}{8\pi v_0 \sin(\theta/2)}, \quad \alpha_1 = \alpha_0 \frac{w_{AA}}{w_{AB}}. \quad (4)$$

a_0 and v_0 are, respectively, the monolayer graphene's lattice spacing and the Fermi velocity. w_{AA} and w_{AB} are roughly the hopping amplitudes in the AA and AB/BA stacking regions. In the realistic system, α_0 is expected to be around $\alpha_0 \approx 0.586$ and $\frac{w_{AA}}{w_{AB}}$ is expected to be around $\frac{w_{AA}}{w_{AB}} \approx 0.8$ [43]. Many interesting features related to this noninteracting model have been studied extensively in the past year [47–57].

III. INTERACTION MODEL FOR TBLG

In this paper, we mostly work with a simple yet reasonable model for interactions in TBLG. The effect of more general interactions is discussed later.

We start by considering the RPA screened Coulomb interaction $V(q)$. The exact $V(q)$ has been found to be rather complicated [58]. An approximation for the small q behavior of $V(q)$ can be obtained from simple Thomas-Fermi screening arguments. A rough estimate for the Thomas-Fermi screening wave vector q_{TF} can be obtained from the monolayer-graphene results of Ref. [59] (by using a renormalized Fermi velocity). This result suggest that $G_{\text{moiré}} \ll q_{\text{TF}} \ll G_{\text{graphene}}$. Since $q_{\text{TF}} \ll G_{\text{graphene}}$, in this regime the interaction is independent of layer and sublattice separation (these distances are much smaller than $1/q_{\text{TF}}$). Also the rotation angle θ is small, therefore its effect on interparticle distance can be dropped (interaction becomes layer-independent). Note that the low-energy states included in the continuum model of Bistritzer and Macdonald are only the states close to Dirac points $|k - K| < O(1)G_{\text{moiré}}$. Since $G_{\text{moiré}} \ll q_{\text{TF}}$, in this regime $V(q)$ is effectively constant. Similarly, because $q_{\text{TF}} \ll G_{\text{graphene}}$, the intervalley scattering terms are strongly suppressed and the valley index becomes an effective good quantum number [approximate $U(1)_v$ symmetry]. Putting everything together leads to the following simplified form of the interaction:

$$V = U \sum_q \sum_{(\sigma', v', s', l') \neq (\sigma, v, s, l)} \rho_{\sigma, v, s, l}(q) \rho_{\sigma', v', s', l'}(-q). \quad (5)$$

Here $\rho_{\sigma, v, s, l}(q) = \sum_k c_{\sigma, v, s, l, k+q}^{\dagger} c_{\sigma, v, s, l, k}$ is the density wave operator. σ, v, s, l are the spin, valley, sublattice, and layer indices, respectively. The term with all the indices equal is dropped since it only renormalizes the chemical potential (which is irrelevant at a fixed filling).

IV. FERROMAGNETISM IN THE PERFECTLY FLATBAND LIMIT OF TBLG

Let us now consider the effect of the interaction Eq. (5) on TBLG in the chiral limit [$\alpha_0 = 0.586$ and $\alpha_1 = 0$ in Eq. (3)]. In this limit, the flatband wave functions can be taken to be sublattice polarized [36] so that the sublattice index s is a good quantum number in addition to σ, v . We now have eight

degenerate flatbands that can be labeled by spin, valley, and sublattice indices σ, v, s .

Assuming the interaction parameter U is small compared to the band gap W , we can consider an effective Hamiltonian,

$$H_t = U \sum_{q,l,l',f \neq f'} P_0 \rho_{f,l}(q) P_0 \rho_{f',l'}(-q) P_0, \quad (6)$$

where P_0 is the projection operator into the flatbands, and f refers to the collective σ, v, s . Note that working with this projected Hamiltonian is tantamount to first-order degenerate perturbation theory. This Hamiltonian (that we focus on here) differs from Eq. (5) by ‘‘intraflavor interlayer’’ terms. These terms are omitted here to allow for analytical progress. Later, we will show numerically that these terms do not have a significant effect on the ground state. The projected density operators $P_0 \rho_{f,l}(q) P_0$ in H_t commute with the kinetic energy term in the flatband limit, so that we can ignore the kinetic energy. A spin, valley, and sublattice polarized state corresponding to fully filling one of these bands labeled by $|f = f_0\rangle = \prod_{k \in \text{MBZ}} c_{f_0,k}^\dagger |0\rangle$ is a null state (i.e., zero-energy eigenstate) of H_t . To see this, note that

$$P_0 \rho_{f,l}(q) P_0 |f = f_0\rangle = \sum_{G_{\text{moiré}}} \Lambda_l(G_{\text{moiré}}) \delta_{f,f_0} \delta_{q,G_{\text{moiré}}} |f = f_0\rangle, \quad (7)$$

which implies that

$$H_t |f = f_0\rangle = U \sum_{G_{\text{moiré}}, G'_{\text{moiré}}, l, l', f \neq f'} \Lambda_l(G_{\text{moiré}}) \Lambda_{l'}(G'_{\text{moiré}}) \delta_{f,f_0} \delta_{f',f_0} |f = f_0\rangle = 0. \quad (8)$$

Note that the Hamiltonian in H_t in Eq. (6) is non-negative, i.e., $\langle H_t \rangle \geq 0$. This becomes manifest if we Fourier transform back into ‘‘real’’ space,

$$H_t = U \int d^2\mathbf{r} \sum_{l,l',f \neq f'} [P_0 n_{f,l}(\mathbf{r}) P_0] [P_0 n_{f',l'}(\mathbf{r}) P_0], \quad (9)$$

where $n_{f,l}(\mathbf{r})$ is the real-space density operator. The two parts of each product term commute as they are associated with different values of f . They are also both non-negative as they are projected non-negative operators.

Therefore, the null state $|f = f_0\rangle$ in an exact ground state of H_t at filling is $-3/4$ (one electron per unit cell) of the flatband manifold. Since the chiral limit Hamiltonian is particle-hole symmetric, the same results also hold for the opposite filling fraction $+3/4$. That is, the fully polarized state is an exact ground state at fillings $\pm 3/4$. By assuming a large enough (substrate induced) sublattice potential $\Delta_t = \Delta_b > U$, the same result can be easily generalized to filling fractions $\pm 1/4$. Note that the band-structure properties of TBLG guarantee that all of the ferromagnetic states discussed here are also associated with a quantized anomalous Hall response [39,40,60].

In principle, we can consider spin- or valley-polarized ferromagnetic states at $\pm 1/2$ or 0 (charge-neutrality) fillings. The spin- or valley-polarized states at $\pm 1/2$ or 0 (charge-neutrality) fillings are in fact energy eigenstates as they are the unique maximally spin- or valley-polarized states at the corresponding filling fraction. However, note that for our choice

of interaction, their energy eigenvalues of these states, defined as

$$\begin{aligned} H_t |\sigma = \sigma_0\rangle &= E_\sigma |\sigma = \sigma_0\rangle, \\ H_t |v = v_0\rangle &= E_v |v = v_0\rangle, \end{aligned} \quad (10)$$

are positive, i.e., $E_\sigma, E_v > 0$, as intervalley (for spin-polarized state) or interspin (for valley-polarized state) interaction terms do not vanish in this case. This is in sharp contrast with the flavor-polarized states at $\pm 3/4$, where this energy eigenvalue vanishes identically. Therefore, the flatband approach in this paper does not offer significant insight over mean-field theory at these fillings since it is difficult to rule out non-Slater-determinant states that have lower energies compared to the polarized states E_σ, E_v . However, the mean-field studies of Refs. [61–64] find that the spin-/valley-polarized states are good ground-state candidates even at $\pm 1/2, 0$ filling, but mean field compares energy only between Slater-determinant states and as a result is known to overestimate the prevalence of ferromagnetism in many electronic systems. We further remark that while mean field cannot establish polarized states as ground states, it can certainly rule them out by just finding competing Slater-determinant states with lower energy. While our approach can provide more information about $\pm 3/4$ filling fractions, it cannot be used to make definite statements about the $\pm 1/2$ or 0 (charge-neutrality) fillings without further analysis of H_t . Specifically, further progress can be made by finding a trial state ψ with energy expectation value $\langle \psi | H_t | \psi \rangle < E_{\sigma,v}$ that would rule out polarized states as ground states.

We note that while we did not establish the uniqueness of the ferromagnetic ground state, in the flatband ferromagnetism literature [which is focused on SU(2) ferromagnetism as opposed to the flavor ferromagnetism discussed here] it has been shown [4] that the uniqueness of the ferromagnetic ground state can be established by studying the one-magnon spectrum. A discussion of this point is provided in the Supplemental Material [65]. This puts additional context around the usefulness of the one-magnon spectrum as used in this paper.

V. SPIN STIFFNESS AND THE STABILITY OF FERROMAGNETISM IN TBLG

We now turn to discussing the stability of this ferromagnetic state using the one-magnon spectrum. This is a crucial step as it provides a nontrivial consistency check and allows us to generalize the results of the idealized model [Eq. (6)] to more realistic systems. If the system is truly ferromagnetic, it is necessary but not sufficient for the $q = 0$ state to have the minimum energy [since it is related to the fully polarized state by an SU(2) rotation]. This establishes the ferromagnetic state as the local energy minimum. We note that even though in principle the local stability of the ferromagnetic state is not enough to guarantee global stability, application of our method to a few known examples (in the Supplemental Material [65]) suggests that in practice the ferromagnetic region of the phase diagram can be identified effectively. We can further use the one-magnon band spectrum of the system to obtain useful information such as spin stiffness.

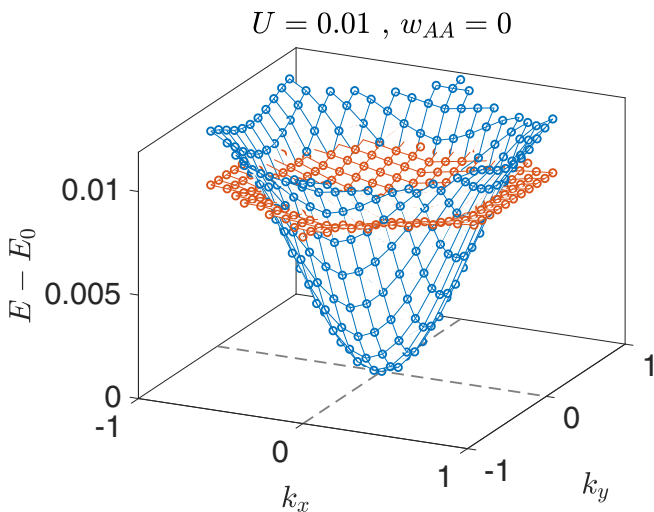


FIG. 1. Lowest one-magnon band spectrum of the TBLG in the chiral limit. Energies are measured with respect to the fully polarized state. The gapless blue curve corresponds to the single-spin flip branch associated with the SU(2) breaking Goldstone mode. The gapped red curve corresponds to the single-valley flip branch associated with breaking the discrete time-reversal symmetry. Energies are in units of $\frac{8\pi v_0 \sin(\theta/2)}{3a_0} \approx 0.19$ eV. k_x and k_y are in units of $\frac{8\pi \sin(\theta/2)}{3a_0}$. We have used the interaction form V [Eq. (5)].

A combination translation invariance and flavor conservation ensures that the one-magnon (single-spin or valley-flip) Hilbert space is small enough to be accessible using exact diagonalization. We use the *exactly* calculated one-magnon spectrum to study the stability of the ferromagnetic state. The exactly calculated band structure of the one-magnon excitations using the interaction V [Eq. (5)] is shown in Fig. 1. The blue curve corresponds to the single-spin flip branch of excitations associated with the SU(2) breaking Goldstone mode. The red curve corresponds to the single-valley flip branch of excitations associated with breaking of the time-reversal symmetry. Importantly, note that since time-reversal symmetry is discrete, the single-valley flip excitations are gapped. As shown in Fig. 1, the ferromagnetic state is stable in this case.

The numerical stability of the ferromagnetic state shows that the “intraflavor interlayer” terms

$$\Delta H_t = 2U \sum_q \sum_f P_0 \rho_{f,l=1}(q) P_0 \rho_{f,l=2}(-q) P_0 \quad (11)$$

that were ignored in the analytic arguments based on Eq. (6) do not significantly affect the ferromagnetism (we have checked that this term only causes small corrections to the one-magnon spectrum). This term favors layer polarization. However, even approximately layer-polarized states do not exist in the flatband subspace (layer polarization is largely fixed by the noninteracting flatband wave functions). Additionally, such terms constitute a combinatorially small fraction $1/28$ of the total terms of Eq. (5). Adding this term to Eq. (6) can be thought of as deviating from the ideal interaction form of Eq. (6) toward the more realistic interaction in Eq. (5).

We now deviate from the chiral limit and proceed to study the stability of the ferromagnetic state as the realistic system is approached. For simplicity, here we assume

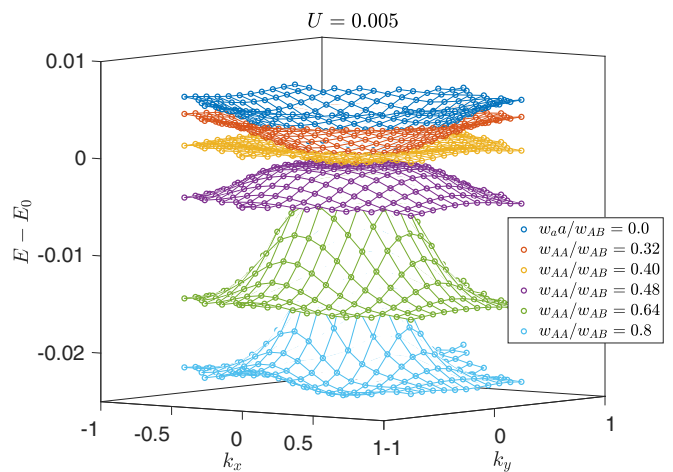


FIG. 2. Lowest one-magnon (single spin-flip) band spectrum of the TBLG as the realistic system is approached. Energies are measured with respect to the fully polarized state in the chiral limit. Energies are in units of $\frac{8\pi v_0 \sin(\theta/2)}{3a_0} \approx 0.19$ eV. Here $\Delta_t = \Delta_b = 0.1 \approx 18$ meV. k_x and k_y are in units of $\frac{8\pi \sin(\theta/2)}{3a_0}$. We have used the interaction form V [Eq. (5)].

a substrate-induced sublattice potential $\Delta_t = \Delta_b = 0.1 \approx 18$ meV. This assumption gaps one of the flatbands and helps with the computational complexity. We numerically calculate the one-magnon (single spin-flip) spectrum as we approach the realistic parameters $w_{AA}/w_{AB} = 0.8$ [43]. The instability of the ferromagnetic state is identified by a sign change of the spin stiffness, or more precisely by looking for one-magnon states whose energy is lower than the ferromagnetic state. Sample results are shown in Fig. 2. In Fig. 2 we have set $U = 0.005 \approx 1$ meV. As shown in the figure, as the realistic parameters are approached, the ferromagnetic state becomes unstable. To study this transition more carefully, we have plotted the calculated value of spin stiffness ρ_s as a function of w_{AA}/w_{AB} for three different values of U in Fig. 3. ρ_s is extracted assuming $E = \rho_s |k|^2$. Note that as the instability is approached, the spectrum sometimes does not admit a good quadratic fit. Still, the extracted value can be used to see the general trend. As shown in Fig. 3, depending on the value of U , the realistic system can be either ferromagnetic or not. That is, for large enough U , in the realistic parameter regime, the ferromagnetic state is stable. Within the parameter regime used here, we estimate the critical value of U_c to be around $U_c \approx 2$ meV.

Before ending this section, we would like to emphasize that our formalism can be applied to *arbitrary* interaction models, and that the model considered here only provides an example that can be generalized to more complicated models in future work.

VI. DISCUSSION AND CONCLUSION

In this paper, we have shown that a simple variant of the ideas related to flatband ferromagnetism can be used to study TBLG. In particular, we discussed ferromagnetism in the perfectly flatband “chiral” limit, and we used the exactly calculated one-magnon spectrum to study the stability of the

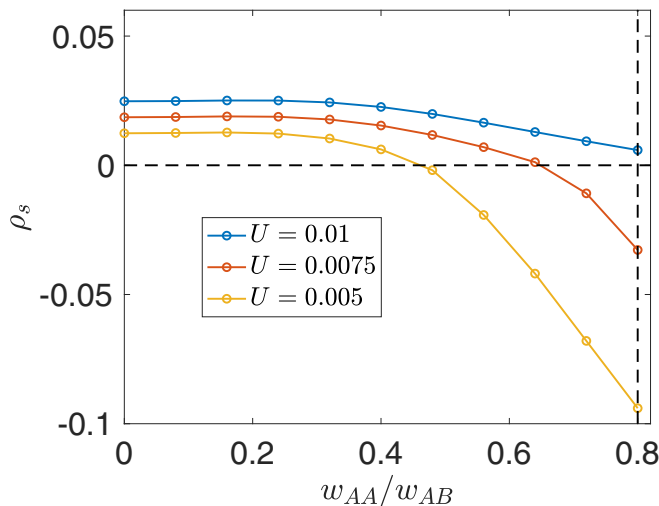


FIG. 3. Spin stiffness associated with the one-magnon band spectrum of the TBLG. A negative spin stiffness signals the instability of the ferromagnetic state. We have used a fit of the form $E = \rho_s |k|^2$. We have used the interaction form V [Eq. (5)].

ferromagnetic state as the realistic system is approached. The same one-magnon spectrum is also used to extract the spin stiffness of the ferromagnetic Goldstone modes. Note that our formalism can be used to study ferromagnetism in other recently discovered ferromagnetic phases in moiré superlattices. In particular, the same exact method can be readily applied to twisted double bilayer graphene where an analogous chiral flat limit exists [38].

A particularly intriguing feature of the results presented here is that (as opposed to the mean-field approach [61–63]) they manifestly predict ferromagnetism *only* at odd filling fractions $\pm 3/4, 1/4$. Given that the experimentally observed half-filled state seems to be spin-unpolarized [23–25], it would be interesting to study the fate of the model presented here at half-filling and to see if it also hosts a spin-unpolarized ground state.

The exactly calculated one-magnon spectrum studied here can be used to extract other interesting information about the ferromagnetic state. In particular, the Chern insulating nature of the ferromagnetic states means that the spin stiffness can be used to calculate the energy of charged skyrmions [66–71].

The skyrmion energy in combination with the Hartree-Fock particle hole excitation energy can then be used to determine whether skyrmions are the lowest-lying charged excitations (note that even in Landau levels, this is not always the case). This result can be compared with experimentally measured charge gaps of Ref. [35]. We further remark that the one-magnon spectrum can also be used to identify natural candidates for the neighboring magnetic phases. Specifically, when the ferromagnetic state becomes unstable, i.e., when the minima of the one-magnon spectrum has finite momentum $q_0 \neq 0$, the location of the new minima in the Brillouin zone can be used to identify natural candidates for alternate types of magnetic order (e.g., antiferromagnetism) that might replace ferromagnetism in neighboring phases.

We finally mention that the formalism developed here provides an intuitive picture of how ferromagnets are favored over competing Mott insulators in topologically nontrivial bands. Traditionally, when short-range Hubbard interactions are considered, Mott-insulating states are considered as candidate ground states. The idea is to restrict the electrons to sharply localized nonoverlapping Wannier wave functions to minimize the interaction energy. However, note that for nonisolated or isolated and topologically nontrivial bands, Wannier wave functions are not even approximately localized. Therefore, in these cases (overlapping or topologically nontrivial band), Mott-insulating states are not good ground-state candidates, whereas the ferromagnetic states discussed above are good candidates independent of the (topological) nature of the underlying band. In continuation of these ideas, we mention here that the recent experimental finding of Ref. [33] in ABC trilayer graphene, where the Chern number of the band can be electrically tuned, seems to suggest that the topology of the underlying band might in fact play a role in favoring ferromagnetism. Studying this case with the same formalism provides another interesting line of future work.

Note added. During the final stages of preparing this manuscript we became aware of Ref. [72], which also studies ferromagnetism in flatband systems and has some overlap with the present work.

ACKNOWLEDGMENTS

This work was supported by the NSF-DMR1555135 (CAREER), JQI-NSF-PFC (PHY1430094), and the Sloan research fellowship. We acknowledge the support of the University of Maryland supercomputing resources.

-
- [1] G. Mahan (unpublished).
 - [2] J. Kanamori, *Prog. Theor. Phys.* **30**, 275 (1963).
 - [3] J. Stöhr and H. C. Siegmann, *Solid-State Sciences* (Springer, Berlin, 2006), Vol. 5.
 - [4] A. Mielke, *Phys. Lett. A* **174**, 443 (1993).
 - [5] J. Hubbard and B. H. Flowers, *Proc. R. Soc. London, Ser. A* **276**, 238 (1963).
 - [6] Y. Nagaoka, *Phys. Rev.* **147**, 392 (1966).
 - [7] D. J. Thouless, *Proc. Phys. Soc.* **86**, 893 (1965).
 - [8] H. Tasaki, *Phys. Rev. B* **40**, 9192 (1989).
 - [9] E. H. Lieb, *Phys. Rev. Lett.* **62**, 1201 (1989).
 - [10] H. Tasaki, *J. Stat. Phys.* **84**, 535 (1996).
 - [11] A. Mielke, *J. Phys. A* **24**, L73 (1991).
 - [12] A. Mielke, *J. Phys. A* **24**, 3311 (1991).
 - [13] A. Mielke, *J. Phys. A* **25**, 4335 (1992).
 - [14] A. Mielke and H. Tasaki, *Commun. Math. Phys.* **158**, 341 (1993).
 - [15] H. Tasaki, *Phys. Rev. Lett.* **69**, 1608 (1992).
 - [16] H. Tasaki, *Phys. Rev. Lett.* **73**, 1158 (1994).
 - [17] H. Tasaki, *Phys. Rev. Lett.* **75**, 4678 (1995).

- [18] H. Tasaki, *Prog. Theor. Phys.* **99**, 489 (1998).
- [19] H. Katsura, I. Maruyama, A. Tanaka, and H. Tasaki, *Europhys. Lett.* **91**, 57007 (2010).
- [20] H. Tasaki, *Eur. Phys. J. B* **64**, 365 (2008).
- [21] A. Tanaka and H. Tasaki, *Phys. Rev. Lett.* **98**, 116402 (2007).
- [22] B. Hunt, J. D. Sanchez-Yamagishi, A. F. Young, M. Yankowitz, B. J. LeRoy, K. Watanabe, T. Taniguchi, P. Moon, M. Koshino, P. Jarillo-Herrero, and R. C. Ashoori, *Science* **340**, 1427 (2013).
- [23] Y. Cao, V. Fatemi, S. Fang, K. Watanabe, T. Taniguchi, E. Kaxiras, and P. Jarillo-Herrero, *Nature (London)* **556**, 43 (2018).
- [24] Y. Cao, V. Fatemi, A. Demir, S. Fang, S. L. Tomarken, J. Y. Luo, J. D. Sanchez-Yamagishi, K. Watanabe, T. Taniguchi, E. Kaxiras, R. C. Ashoori, and P. Jarillo-Herrero, *Nature (London)* **556**, 80 (2018).
- [25] M. Yankowitz, S. Chen, H. Polshyn, Y. Zhang, K. Watanabe, T. Taniguchi, D. Graf, A. F. Young, and C. R. Dean, *Science* **363**, 1059 (2019).
- [26] A. Kerelsky, L. McGilly, D. M. Kennes, L. Xian, M. Yankowitz, S. Chen, K. Watanabe, T. Taniguchi, J. Hone, C. Dean, A. Rubio, and A. N. Pasupathy, *Nature (London)* **572**, 95 (2019).
- [27] Y. Choi, J. Kemmer, Y. Peng, A. Thomson, H. Arora, R. Polski, Y. Zhang, H. Ren, J. Alicea, G. Refael, F. von Oppen, K. Watanabe, T. Taniguchi, and S. Nadj-Perge, *Nat. Phys.* **15**, 1174 (2019).
- [28] A. L. Sharpe, E. J. Fox, A. W. Barnard, J. Finney, K. Watanabe, T. Taniguchi, M. A. Kastner, and D. Goldhaber-Gordon, *Science* **365**, 605 (2019).
- [29] S. Moriyama, Y. Morita, K. Komatsu, K. Endo, T. Iwasaki, S. Nakaharai, Y. Noguchi, Y. Wakayama, E. Watanabe, D. Tsuya, K. Watanabe, and T. Taniguchi, *arXiv:1901.09356*.
- [30] X. Lu, P. Stepanov, W. Yang, M. Xie, M. A. Aamir, I. Das, C. Urgell, K. Watanabe, T. Taniguchi, G. Zhang, A. Bachtold, A. H. MacDonald, and D. K. Efetov, *Nature (London)* **574**, 653 (2019).
- [31] C. Shen, Yanbang Chu, Quan Sheng Wu, N. Li, S. Wang, Y. Zhao, J. Tang, J. Liu, J. Tian, K. Watanabe, T. Taniguchi, R. Yang, Z. Y. Meng, D. Shi, O. V. Yazyev, and G. Zhang, *Nat. Phys.* **116**, 520 (2020).
- [32] X. Liu, Z. Hao, E. Khalaf, J. Y. Lee, K. Watanabe, T. Taniguchi, A. Vishwanath, and P. Kim, *Nature (London)* **583**, 221 (2020).
- [33] G. Chen, A. L. Sharpe, E. J. Fox, Y.-H. Zhang, S. Wang, L. Jiang, B. Lyu, H. Li, K. Watanabe, T. Taniguchi, Z. Shi, T. Senthil, D. Goldhaber-Gordon, Y. Zhang, and F. Wang, *Nature* **579**, 56 (2020).
- [34] Y. Cao, D. Rodan-Legrain, O. Rubies-Bigorda, J. M. Park, K. Watanabe, T. Taniguchi, and P. Jarillo-Herrero, *Nature* **583**, 215 (2020).
- [35] M. Serlin, C. L. Tschirhart, H. Polshyn, Y. Zhang, J. Zhu, K. Watanabe, T. Taniguchi, L. Balents, and A. F. Young, *Science* **367**, 900 (2020).
- [36] G. Tarnopolsky, A. J. Kruchkov, and A. Vishwanath, *Phys. Rev. Lett.* **122**, 106405 (2019).
- [37] E. Khalaf, A. J. Kruchkov, G. Tarnopolsky, and A. Vishwanath, *Phys. Rev. B* **100**, 085109 (2019).
- [38] F. Haddadi, Q. S. Wu, A. J. Kruchkov, and O. V. Yazyev, *Nano Lett.* **20**, 2410 (2020).
- [39] Y.-H. Zhang, D. Mao, and T. Senthil, *Phys. Rev. Research* **1**, 033126 (2019).
- [40] N. Bultinck, S. Chatterjee, and M. P. Zaletel, *Phys. Rev. Lett.* **124**, 166601 (2020).
- [41] R. Bistritzer and A. H. MacDonald, *Proc. Natl. Acad. Sci. (USA)* **108**, 12233 (2011).
- [42] J. M. B. Lopes dos Santos, N. M. R. Peres, and A. H. Castro Neto, *Phys. Rev. B* **86**, 155449 (2012).
- [43] M. Koshino, N. F. Q. Yuan, T. Koretsune, M. Ochi, K. Kuroki, and L. Fu, *Phys. Rev. X* **8**, 031087 (2018).
- [44] M. Yankowitz, J. Jung, E. Laksono, N. Leconte, B. L. Chittari, K. Watanabe, T. Taniguchi, S. Adam, D. Graf, and C. R. Dean, *Nature (London)* **557**, 404 (2018).
- [45] A. A. Zibrov, E. M. Spanton, H. Zhou, C. Kometter, T. Taniguchi, K. Watanabe, and A. F. Young, *Nat. Phys.* **14**, 930 (2018).
- [46] H. Kim, N. Leconte, B. L. Chittari, K. Watanabe, T. Taniguchi, A. H. MacDonald, J. Jung, and S. Jung, *Nano Lett.* **18**, 7732 (2018).
- [47] H. C. Po, L. Zou, A. Vishwanath, and T. Senthil, *Phys. Rev. X* **8**, 031089 (2018).
- [48] N. F. Q. Yuan and L. Fu, *Phys. Rev. B* **98**, 045103 (2018).
- [49] H. C. Po, H. Watanabe, and A. Vishwanath, *Phys. Rev. Lett.* **121**, 126402 (2018).
- [50] H. C. Po, L. Zou, T. Senthil, and A. Vishwanath, *Phys. Rev. B* **99**, 195455 (2019).
- [51] K. Hejazi, C. Liu, H. Shapourian, X. Chen, and L. Balents, *Phys. Rev. B* **99**, 035111 (2019).
- [52] Z. Song, Z. Wang, W. Shi, G. Li, C. Fang, and B. A. Bernevig, *Phys. Rev. Lett.* **123**, 036401 (2019).
- [53] S. Carr, S. Fang, Z. Zhu, and E. Kaxiras, *Phys. Rev. Research* **1**, 013001 (2019).
- [54] Z. Ma, S. Li, Y.-W. Zheng, M.-M. Xiao, H. Jiang, J.-H. Gao, and X. C. Xie, *arXiv:1905.00622*.
- [55] E. H. Hwang and S. D. Sarma, *Phys. Rev. Research* **2**, 013342 (2020).
- [56] F. Wu, E. Hwang, and S. Das Sarma, *Phys. Rev. B* **99**, 165112 (2019).
- [57] J. Kang and O. Vafek, *Phys. Rev. X* **8**, 031088 (2018).
- [58] J. M. Pizarro, M. Rösner, R. Thomale, R. Valentí, and T. O. Wehling, *Phys. Rev. B* **100**, 161102 (2019).
- [59] E. H. Hwang and S. Das Sarma, *Phys. Rev. B* **75**, 205418 (2007).
- [60] Y.-H. Zhang, D. Mao, Y. Cao, P. Jarillo-Herrero, and T. Senthil, *Phys. Rev. B* **99**, 075127 (2019).
- [61] M. Xie and A. H. MacDonald, *Phys. Rev. Lett.* **124**, 097601 (2020).
- [62] S. Liu, E. Khalaf, J. Y. Lee, and A. Vishwanath, *arXiv:1905.07409*.
- [63] F. Wu and S. D. Sarma, *Phys. Rev. B* **101**, 155149 (2020).
- [64] J. Kang and O. Vafek, *Phys. Rev. Lett.* **122**, 246401 (2019).
- [65] See Supplemental Material at <http://link.aps.org/supplemental/10.1103/PhysRevB.102.235123> for detailed calculations on simple models as well as an expanded discussion of flat-band ferromagnetism.
- [66] S. L. Sondhi, A. Karlhede, S. A. Kivelson, and E. H. Rezayi, *Phys. Rev. B* **47**, 16419 (1993).
- [67] K. Yang, K. Moon, L. Zheng, A. H. MacDonald, S. M. Girvin, D. Yoshioka, and S.-C. Zhang, *Phys. Rev. Lett.* **72**, 732 (1994).
- [68] K. Moon, H. Mori, K. Yang, S. M. Girvin, A. H. MacDonald, L. Zheng, D. Yoshioka, and S.-C. Zhang, *Phys. Rev. B* **51**, 5138 (1995).

- [69] D. P. Arovas, A. Karlhede, and D. Lilliehöök, [Phys. Rev. B **59**, 13147 \(1999\)](#).
- [70] J. Alicea and M. P. A. Fisher, [Phys. Rev. B **74**, 075422 \(2006\)](#).
- [71] K. Yang, S. Das Sarma, and A. H. MacDonald, [Phys. Rev. B **74**, 075423 \(2006\)](#).
- [72] C. Repellin, Z. Dong, Y.-H. Zhang, and T. Senthil, [Phys. Rev. Lett. **124**, 187601 \(2020\)](#).